

ARTICLE


<https://doi.org/10.1038/s41467-021-21639-w>

OPEN

Immunogenicity and protective efficacy of inactivated SARS-CoV-2 vaccine candidate, BBV152 in rhesus macaques

Pragya D. Yadav¹, Raches Ella², Sanjay Kumar³, Dilip R. Patil¹, Sreelekshmy Mohandas¹, Anita M. Shete¹, Krishna M. Vadrevu², Gaurav Bhati⁴, Gajanan Sapkal¹, Himanshu Kaushal¹, Savita Patil¹, Rajlaxmi Jain¹, Gururaj Deshpande¹, Nivedita Gupta⁵, Kshitij Agarwal⁵, Mangesh Gokhale¹, Basavaraj Mathapati¹, Siddhanath Metkari⁶, Chandrashekhhar Mote⁷, Dimpal Nyayanit¹, Deepak Y. Patil¹, B. S. Sai Prasad², Annasaheb Suryawanshi¹, Manoj Kadam¹, Abhimanyu Kumar¹, Sachin Daigude¹, Sanjay Gopale¹, Triparna Majumdar¹, Deepak Mali¹, Prasad Sarkale¹, Shreekanth Baradkar¹, Pranita Gawande¹, Yash Joshi¹, Sidharam Fulari¹, Hitesh Dighe¹, Sharda Sharma¹, Rashmi Gunjekar¹, Abhinendra Kumar¹, Kaumudi Kalele¹, Vellimedu K. Srinivas², Raman R. Gangakhedkar⁵, Krishna M. Ella², Priya Abraham¹, Samiran Panda⁵ & Balram Bhargava⁵✉

The COVID-19 pandemic is a global health crisis that poses a great challenge to the public health system of affected countries. Safe and effective vaccines are needed to overcome this crisis. Here, we develop and assess the protective efficacy and immunogenicity of an inactivated SARS-CoV-2 vaccine in rhesus macaques. Twenty macaques were divided into four groups of five animals each. One group was administered a placebo, while three groups were immunized with three different vaccine candidates of BBV152 at 0 and 14 days. All the macaques were challenged with SARS-CoV-2 fourteen days after the second dose. The protective response was observed with increasing SARS-CoV-2 specific IgG and neutralizing antibody titers from 3rd-week post-immunization. Viral clearance was observed from bronchoalveolar lavage fluid, nasal swab, throat swab and lung tissues at 7 days post-infection in the vaccinated groups. No evidence of pneumonia was observed by histopathological examination in vaccinated groups, unlike the placebo group which exhibited interstitial pneumonia and localization of viral antigen in the alveolar epithelium and macrophages by immunohistochemistry. This vaccine candidate BBV152 has completed Phase I/II (NCT04471519) clinical trials in India and is presently in phase III, data of this study substantiates the immunogenicity and protective efficacy of the vaccine candidates.

A full list of author affiliations appears at the end of the paper.

The pandemic of coronavirus disease 2019 (COVID-19) has caused an unprecedented public health burden in several countries across the globe¹. The spread of severe acute respiratory syndrome coronavirus-2 (SARS-CoV-2) is humongous affecting more than 75 million people till December 20, 2020². With all the public health interventions in place including behavioural modifications such as the use of mask, hand sanitisation and social distancing, pharmaceutical interventions such as antiviral drugs or vaccines seem to be the only means of stopping this raging pandemic. With the release of the first genome sequence of SARS-CoV-2 from China on 11 January 2020, the race against the virus and time had begun for the development of an effective COVID-19 vaccine. Multiple vaccine development platforms from traditional to next-generation approaches are being used by different research groups worldwide. Purified inactivated viruses have been traditionally used in vaccine development. The inactivated vaccines have been proven to be safe and effective in the prevention of diseases like rabies, polio, hepatitis A and influenza³. Production of inactivated vaccine is relatively easy and the speed, with which it can be made, makes it a promising strategy for vaccine development for COVID-19⁴. Earlier experience of inactivated vaccine manufacturing and the availability of a BSL-3 facility equipped with a well-characterised Vero cell manufacturing platform aided us in the rapid development of an inactivated vaccine candidate. Moreover, two similar inactivated SARS-CoV-2 candidates based on alum adjuvant, i.e., PiCoVacc and BBIPCoV, have shown encouraging results in non-human primate (NHP) models and have progressed to the human clinical trials^{5,6}.

The safety and the immunogenicity of inactivated vaccine candidate BBV152 has been established in mice, rat and rabbit models⁷. The vaccine candidate has been found to induce an effective humoral immune response and protects Syrian hamsters from SARS-CoV-2 pneumonia⁸. Here, we report the assessment of immunogenicity and protective efficacy of three formulations of a purified whole-virion-inactivated SARS-CoV-2 vaccine candidate BBV152 in the rhesus macaques.

Results

Anti-SARS-CoV-2 IgG and neutralising antibody response. Adverse events were not seen in animals immunised with a two-dose vaccination regimen. We evaluated anti-SARS-CoV-2 immunoglobulin-G (IgG) antibody and neutralising antibody (NAb) titres from the serum samples during the immunisation phase on 0, 12, 19, 26 and 28 days and after SARS-CoV-2 infection on 0, 1, 3, 5 and 7 days post infection (DPI) (Fig. 1a). Using inactivated SARS-CoV-2 IgG antibody detection ELISA, IgG levels were detectable from 3rd week post immunisation and were found increasing till 35th day (7 DPI) (Fig. 1b, c). Group III animals showed the highest IgG titre (1:25,600) compared to groups II and IV (1:1600–1:6400) (Fig. 1d).

Anti-SARS-CoV-2 IgG specific to RBD protein showed a high level of antibody response in the vaccinated group at 28th day post immunisation and 7 DPI (Fig. 1e). Group III showed the highest titre of RBD IgG antibody (1:1600) compared to groups II (1:400) and IV (1:400–1:1600). Similarly, N protein-based ELISA indicated higher IgG titre (1:6400) in Group III as compared to groups II (1:400–1:6400) and IV (1:1600–1:6400) (Fig. 1f).

The highest NAb titres of 1:209–1:5217 were detected in group III after the SARS-CoV-2 challenge. The NAb titres for groups II and IV were (1:87.4–1:3974) and (1:29.5–72 h:3403), respectively (Fig. 2a, b). These NAb titres correlated with the IgG antibody titres. NAb and IgG response was not detectable in the placebo group. Both homologous and heterologous SARS-CoV-2 strains (Q-100 and Q-111) were found to be neutralised by the macaque serum samples collected on 7 DPI (Fig. 2c).

Viral load in the nasal swab, throat swab and bronchoalveolar lavage fluid. Genomic RNA (gRNA) was detected from nasal swab (NS) specimens of all animals in the placebo group from 1 to 7 DPI. Viral clearance was observed in NS specimens of all the animals from vaccinated groups on 7 DPI (Fig. 3a).

Throat swab (TS) specimens of the placebo group were tested positive for gRNA at 1, 3, 5 and 7 DPI. Vaccinated groups had a detectable level of gRNA from 1 to 5 DPI with complete viral clearance on 7 DPI (Fig. 3b). Bronchoalveolar lavage (BAL) fluid specimens of the animals from the placebo group were positive for gRNA from 1 to 7 DPI. In the vaccinated groups, gRNA was detected in BAL specimens until 3 DPI (Fig. 3c). Except for the placebo group, none of the vaccinated groups showed the presence of gRNA in lung lobes in necropsy tissue (Fig. 3d). The comparisons of viral copy numbers of the NS, TS and the BAL fluid samples of the vaccinated as compared to the placebo group were found to be statistically significant using the two-tailed Mann–Whitney test.

Subgenomic RNA was detected in the BAL fluid of 4/5 animals of the placebo animals, whereas it was negative for all the vaccinated animals at 7 DPI (Fig. 4a). In the necropsy specimens of lung tissue at 7 DPI, sgRNA was detected in multiple lobes of 4/5 placebo group of animals (three lobes in 1/5, two lobes in 2/5 and one lobe in 1/5 animals), whereas no sgRNA could be detected in the lung tissue of vaccinated animals (Fig. 4b). In the TS of animals of the placebo group, sgRNA was detected in all the animals at 1 DPI, whereas all the vaccinated animals were negative for sgRNA (Fig. 4c). In placebo-group animals, sgRNA was detected in NS of 2/5 animals at 1 DPI, 2/5 at 3 DPI and 1/5 at 7 DPI. In the vaccinated group, there were significantly lower numbers of animals positive for sgRNA in NS even at 1 DPI (Fig. 4d).

The presence of sgRNA in the BAL fluid and lung tissue (at necropsy) of animals from placebo group I at 7 DPI and absence in the vaccinated animals demonstrates the protective efficacy of the vaccine candidates.

Viral load in the respiratory tract, lungs and extrapulmonary organs. On 7 DPI, animals from all the groups were sacrificed and swab samples, BAL fluid and various organs were collected. In the placebo group, gRNA was detected in the trachea (3/5), nasopharyngeal mucosa (2/5), oropharyngeal mucosa (3/5) and nasal mucosa (1/5) specimens (Fig. 5c). Four out of five animals of the placebo group had detectable gRNA and sgRNA in multiple lobes of lungs (Figs. 5d and 4b). Lung specimens of all animals from the vaccinated groups were found negative for gRNA and sgRNA. In the placebo group, gRNA was detected in the skin, ileum, colon, gall bladder, stomach, urinary bladder and pancreas. Only one animal from group IV showed the presence of gRNA in ileum and caecum, but it was negative for sgRNA. The heart, liver, kidney, spleen and brain were tested negative for gRNA and sgRNA in all animals (Fig. 5e).

Clinicoradiological analysis. Weight loss, pyrexia, worsening of SpO₂ at room air, lethargy, reduced food/water intake and reduced self-grooming were observed in the placebo group, which persisted till 7 DPI, whereas these features resolved in the other groups II and IV (Supplementary Fig. 1 and Supplementary Table 1). Chest radiograph of the three animals in the placebo group showed infiltrates that are suggestive of bronchopneumonia/lobar pneumonia that persisted till 7 DPI. Similarly, chest radiographic abnormalities were detected in two out of five animals in groups II and IV, but resolved by 5 DPI (Supplementary Fig. 2a–d). No clinical or radiographic abnormalities were detected in group III animals.

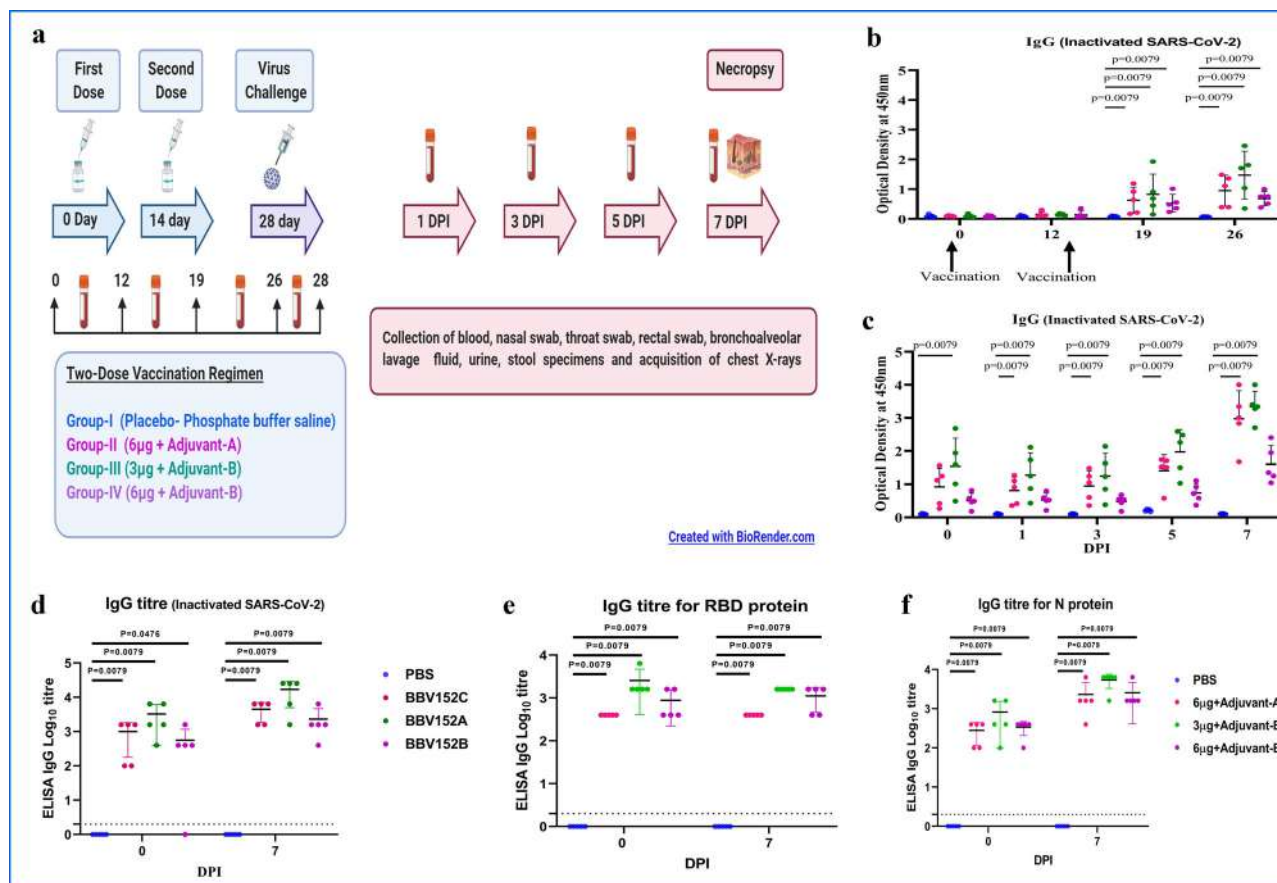


Fig. 1 Experimental summary and IgG response in vaccinated animals. **a** Diagrammatic representation of experiment summary. **b** Anti-SARS-CoV-2 IgG response in animals from 1st to 4th week of immunisation with whole virus-inactivated protein ELISA. **c** Anti-SARS-CoV-2 IgG response at 0, 1, 3, 5 and 7 DPI. **d** Anti-SARS-CoV-2 IgG titres in animals at 0 and 7 DPI. **e** IgG titres for SARS-CoV-2 RBD protein in animals at 0 and 7 DPI. **f** IgG titres for SARS-CoV-2 nucleoprotein in animals at 0 and 7 DPI. The statistical significance was assessed using the Kruskal-Wallis test followed by the two-tailed Mann-Whitney test between two groups; P values of < 0.05 were considered to be statistically significant. The dotted line on the figures indicates the limit of detection of the assay. Data are presented as mean values \pm standard deviation (SD). Statistical comparison was done by comparing the vaccinated group with the placebo group as a control. Group I = blue, group II = pink, group III = green and group IV = purple, number of animals = 5 animals in each group. Source data are provided as a Source Data file.

Histopathological examination and immunohistochemistry.

The gross pathology of the lungs of animals of the placebo group at 7 DPI showed a significantly higher incidence of bronchopneumonic patches and consolidation at necropsy, as compared to the vaccinated groups (Fig. 5a, b). Lung tissues showed moderate-to-severe interstitial pneumonia in the animals of the placebo group (Supplementary Table 2) characterised by thickening of alveolar septa, hyaline membrane formation, accumulation of oedematous fluid and fibrin. Occasionally, certain foci of bronchioles showed necrosis and loss of epithelium with neutrophils and macrophage infiltration (Fig. 6a). Moderate-to-severe disease was present in 3/5 and mild disease in 2/5 animals of the placebo group with the involvement of two to six lung lobes. In group II, 2/5 animals had a single lobe of the lung showing focal mononuclear infiltration (Supplementary Table 3). Lungs of all the other animals of groups II, III and IV appeared normal on histopathology (Fig. 6b–d). Viral antigens were detected in the alveolar epithelium by immunohistochemistry (IHC) in the placebo group suggestive of SARS-CoV-2 infection (Fig. 6e), whereas similar findings were not present in the vaccinated group animals. These findings indicate significant protection of the lungs of the vaccinated group compared to the placebo group (Fig. 6f–h). Groups II, III and IV had significantly lower disease burden compared to the placebo group (Supplementary Tables 2 and 3).

Virus isolation. NS, TS, BAL fluid, urine, stool and lung tissue specimens from placebo (1–7 DPI) and vaccinated groups were processed for virus isolation. Cytopathic effect (CPE) was observed in TS and NS specimens of placebo group on 1 and 3 DPI. BAL, urine, stool and lung specimens did not show CPE in any group. Two TS and one NS specimen of groups II and IV, respectively, yielded virus isolation on 1 DPI.

Lymphocyte subset and cytokine/chemokine profile. Lymphocytes were found to be low in the placebo (mean \pm SD, 14.51 ± 9.31) compared to the vaccinated macaques (group II, mean \pm SD, 31.88 ± 15.85) on 1 DPI. The assessment based on the surface marker of gated lymphocytes from lysed whole blood showed no statistically significant difference between placebo and vaccinated groups in terms of the percentage of cells expressing CD3+ and CD20+ till 7 DPI (extended data, Figs. 3 and Fig. 4). IL-6 was found to be higher in the placebo group (mean \pm SD, 22.78 ± 23.21) compared to groups II (mean \pm SD, 2.97 ± 4.85) and III (mean \pm SD, 2.65 ± 1.98). In addition, the anti-inflammatory cytokine IL-5 was significantly higher in group II (mean \pm SD, 3.14 ± 2.41 , $P < 0.05$) and group III (mean \pm SD, 3.86 ± 3.33 , $P < 0.05$) compared to the placebo group on 1 DPI. IL-8 was found significantly higher in group III on 1 DPI, 3 DPI and 5 DPI (mean \pm SD, 3472 ± 3017 , $P < 0.05$, mean \pm SD, $4653.65 \pm$

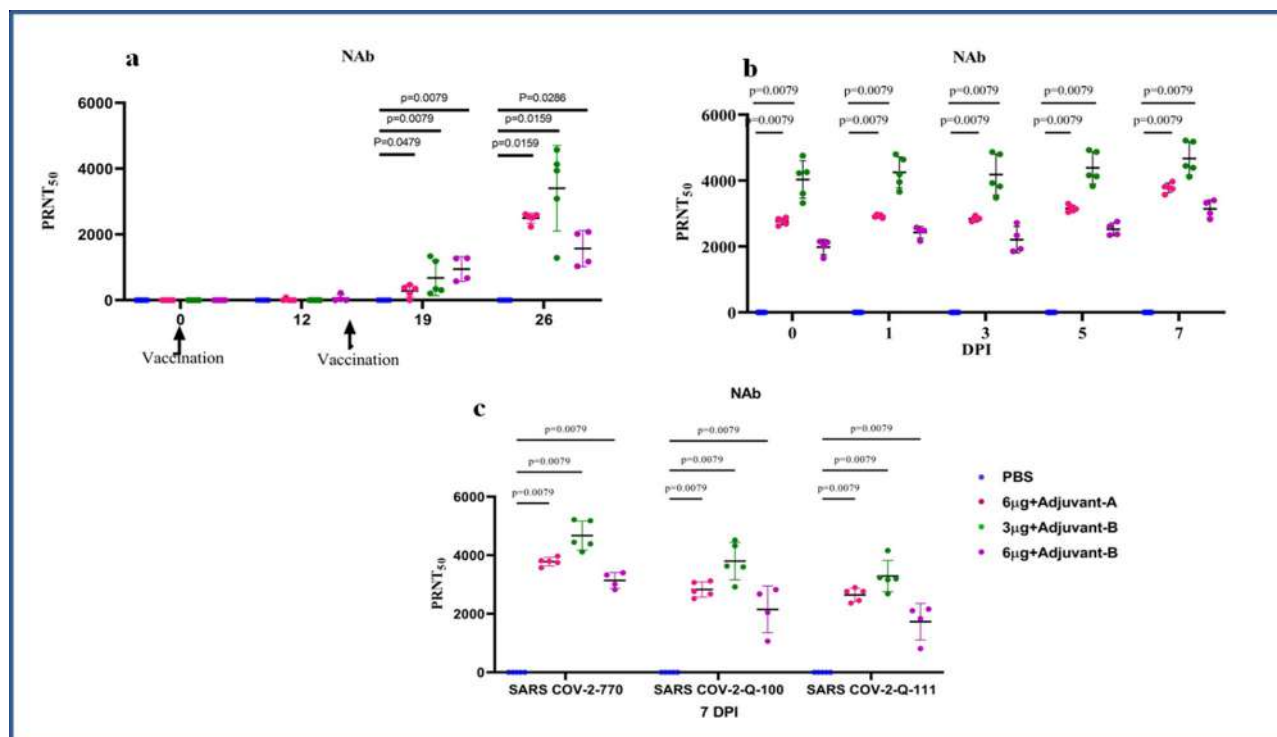


Fig. 2 NAb response in vaccinated animals. **a** NAb titres in animals from 1st to 4th week of immunisation. **b** NAb titres in animals at 0, 1, 3, 5 and 7 DPI. **c** NAb titres in animal samples of 7 DPI with homologous strain 770 and heterologous strain Q-100 and Q-111 of SARS-CoV-2. The statistical significance was assessed using the Kruskal-Wallis test followed by the two-tailed Mann-Whitney test between two groups; *P* values of < 0.05 were considered to be statistically significant. Data are presented as mean values \pm standard deviation (SD). Statistical comparison was done by comparing the vaccinated group with the placebo group as a control. Group I = blue, group II = pink, group III = green and group IV = purple, number of animals = 5 animals in each group. Source data are provided as a Source Data file.

3088.34, $P < 0.05$, mean \pm SD, 4715.5 ± 2864.15 , $P < 0.01$) compared to the placebo group (mean \pm SD, 1891.16 ± 878.11 , 3 DPI, mean \pm SD, 1216.11 ± 757.64 , 5 DPI). IL-2, TNF- α and IFN- γ were not detectable in all the animals (extended data, Fig. 5).

Discussion

A safe and effective vaccine is the need of the hour to overcome the COVID-19 pandemic. In the global race for the development of vaccines, few research groups have reported the preclinical studies of viral vectored vaccines (ChAdOx1 nCoV-19 and Ad-26.COV.2.S)^{9,10}, mRNA vaccine (mRNA-1273)¹¹, DNA vaccine (INO-4800)¹² and inactivated vaccines (PiCoVacc and BBIP-CorV)^{5,6}. Phase III clinical trials have been completed for (mRNA-1273)¹¹ and BNT162b2 (BioNTech/Pfizer)¹³ vaccine candidates and have been granted Emergency Use Authorisation (EUA) by FDA in USA¹⁴. The other vaccine candidates are in the advanced stage of phase III clinical trials. Here, we report the two-dose vaccination regimen of inactivated SARS-CoV-2 vaccine candidates, which was found to induce a strong immune response and protection of animals from the infection of SARS-CoV-2.

NABs and IgG responses were observed from 3rd week post immunisation in vaccinated groups. IgG titres were incremental with the highest response in group III. The presence of sgRNA in NS was observed in the placebo group till 7 DPI. Vaccinated groups had no detectable sgRNA in NS on 7 DPI indicating the ability of vaccine candidates to limit upper respiratory tract viral replication, which is a key factor determining the virus transmission. sgRNA was not detected in the BAL fluid from 5 DPI, suggesting that vaccination hindered virus replication and enabled faster clearance from lower airway protecting the animals. sgRNA was detected in multiple organs at necropsy in the

placebo group, whereas it was found to be cleared in the vaccinated groups.

The presence of sgRNA in the respiratory tissues has been considered as a marker of active replication of the SARS-CoV-2 in the lungs¹⁵. However, Alexandersen et al.¹⁶ has suggested that the detection of sgRNA is not direct evidence of active infection; instead, its presence is just detected at lower levels than virion sgRNA resulting in detection for a shorter period of time. The detection of sgRNA in the tissues will be influenced by the volume of virus challenge dose and the TCID₅₀ value of the virus used for the challenge. In the NHP preclinical studies for SARS-CoV-2 vaccine candidates published showing significant detection of sgRNA, the volumes of virus used during the challenge study have been varying. In ChAdOx1-nCoV NHP challenge study⁹, virus challenge dose used was 6.5 ml and in mRNA-1273 (Moderna) NHP challenge study¹¹ volume of virus used was 4 ml. The protective efficacy of inactivated vaccine candidates BBIP-CorV⁵, PiCoVacc⁶ and BNT162b2, an mRNA vaccine candidate¹³, has been demonstrated in these NHP studies even though sgRNA was not evaluated. In our study, the total volume of virus used for challenge was 1.5 ml (intratracheal 1 ml, intranasal 0.5 ml, TCID₅₀ $10^{6.5}$ /ml). This may explain the lower rate of detection sgRNA in the post-challenge period. However, even with a lower volume of virus used for the challenge, sgRNA was detected in multiple lobes of 4/5 animal in the placebo group in the necropsy specimen of lungs at 7 DPI, while sgRNA was absent in all the animals of the vaccinated group demonstrating the protective efficacy of the vaccine candidates.

Another factor that needs to be highlighted is the volume of fluid instilled prior to collection of BAL fluid. At 7 DPI, we instilled 10–15 ml of saline to aspirate BAL fluid prior to necropsy

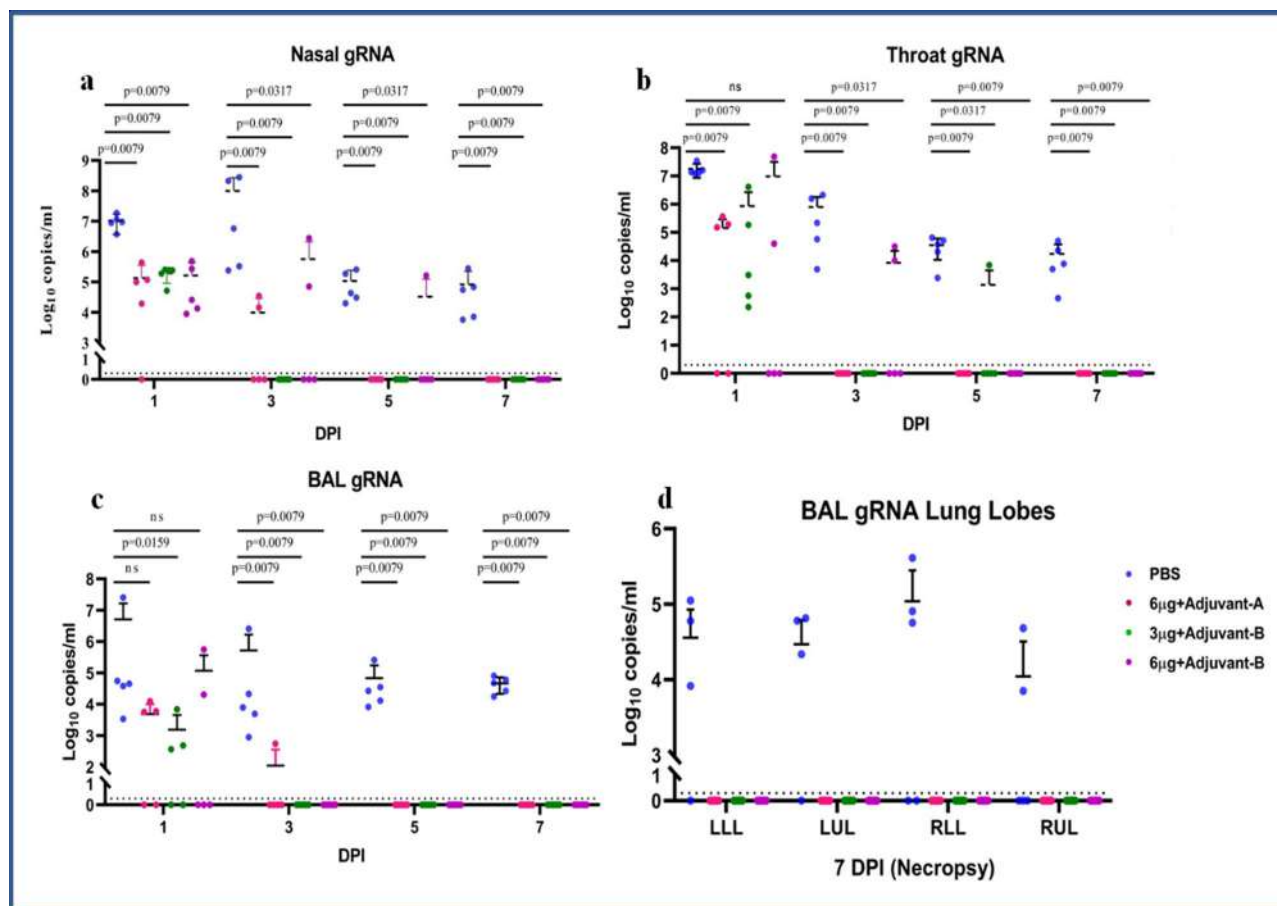


Fig. 3 Genomic viral RNA detection in respiratory tract specimens. Genomic viral RNA load in (a) nasal swab, (b) throat swab and (c) BAL at 1, 3, 5 and 7 DPI. **d** Genomic viral RNA load in different lobes of lungs at 7 DPI. The statistical significance was assessed using the Kruskal-Wallis test followed by the two-tailed Mann-Whitney test between the two groups; P values < 0.05 were considered to be statistically significant. The dotted lines indicate the limit of detection of the assay. Data are presented as mean values \pm standard deviation (SD). Statistical comparison was done by comparing the vaccinated group with the placebo group as a control. Group I = blue, group II = pink, group III = green and group IV = purple, number of animals = 5 animals in each group. Source data are provided as a Source Data file.

and sgRNA was detected in 4/5 animals of the placebo group, while the vaccinated animals had no detection of sgRNA in BAL fluid. In the BAL fluid, aspiration procedure performed at 1, 3 and 5 DPI, we had instilled only 3–5 ml of saline prior to aspiration, which explains the poor detection of the sgRNA in the initial samples. The presence of sgRNA in the BAL fluid at 7 DPI and lung tissue at necropsy of the animals in the placebo group and absence in the vaccinated groups demonstrates the protective efficacy of the vaccine candidates investigated in this study.

Wang et al. and colleagues reported immunogenicity of the two-dose vaccination regimen with effective NAb response in low and middle vaccine doses of inactivated SARS-CoV-2 vaccine and noted virus clearance⁵. Similarly, Gao et al. and colleagues also reported rising titres of NAb with three dose vaccination regimen and protection of animals by virus clearance from the pharynx or lungs at 7 DPI with high vaccine dose⁶.

An elevated level of IL-6 is highly consistent in COVID-19 disease and lymphopenia may be associated with a high level of IL-6^{17,18}. Our experimental data showed an elevated level of IL-6 in the placebo group compared to vaccinated groups (II and III) on 1 DPI, suggestive of protection against the SARS-CoV-2 infection. The transient lymphopenia in the placebo group could be suggestive of suboptimal cellular immunity in the placebo group or may be due to the recruitment of lymphocytes to the inflamed respiratory tract^{19,20}. Furthermore, lymphopenia is

specifically CD8⁺ T cells biased^{19,21}, which possibly explains the elevated proportion of CD4⁺ T cells in the placebo group¹⁹. IL-5, a Th₂ cytokine, is associated with eosinophilia and evidence of eosinophils for antiviral activity is documented²². Our study demonstrated a transient increase in serum IL-5 level on 1 DPI in the vaccinated group II, which subsided by 3 DPI. In addition, the haematological data indicated the percentage of eosinophils in the normal range and there were no signs of eosinophilic infiltration in the lungs in the histopathology on the day of sacrifice, indicative of no association with vaccine-enhanced disease. IL-8, a key chemokine, responsible for the recruitment of neutrophils and other immune cells, was substantially high in vaccinated group III indicative of vaccine-induced immune response to infection.

Organ viral load, interstitial pneumonia and detection of viral antigen by IHC in lung tissue strengthens the evidence of SARS-CoV-2-induced pulmonary disease in placebo group animals. Group III (3 µg, adjuvant-A) animals had no clinical/radiological evidence of disease demonstrating significant protection from SARS-CoV-2. These findings correlate well with protection from disease as demonstrated by serological, gross pathological and HPE findings.

This study was performed during the period of countrywide lockdown in India with a complete suspension of international flights because of the pandemic that became detrimental to the

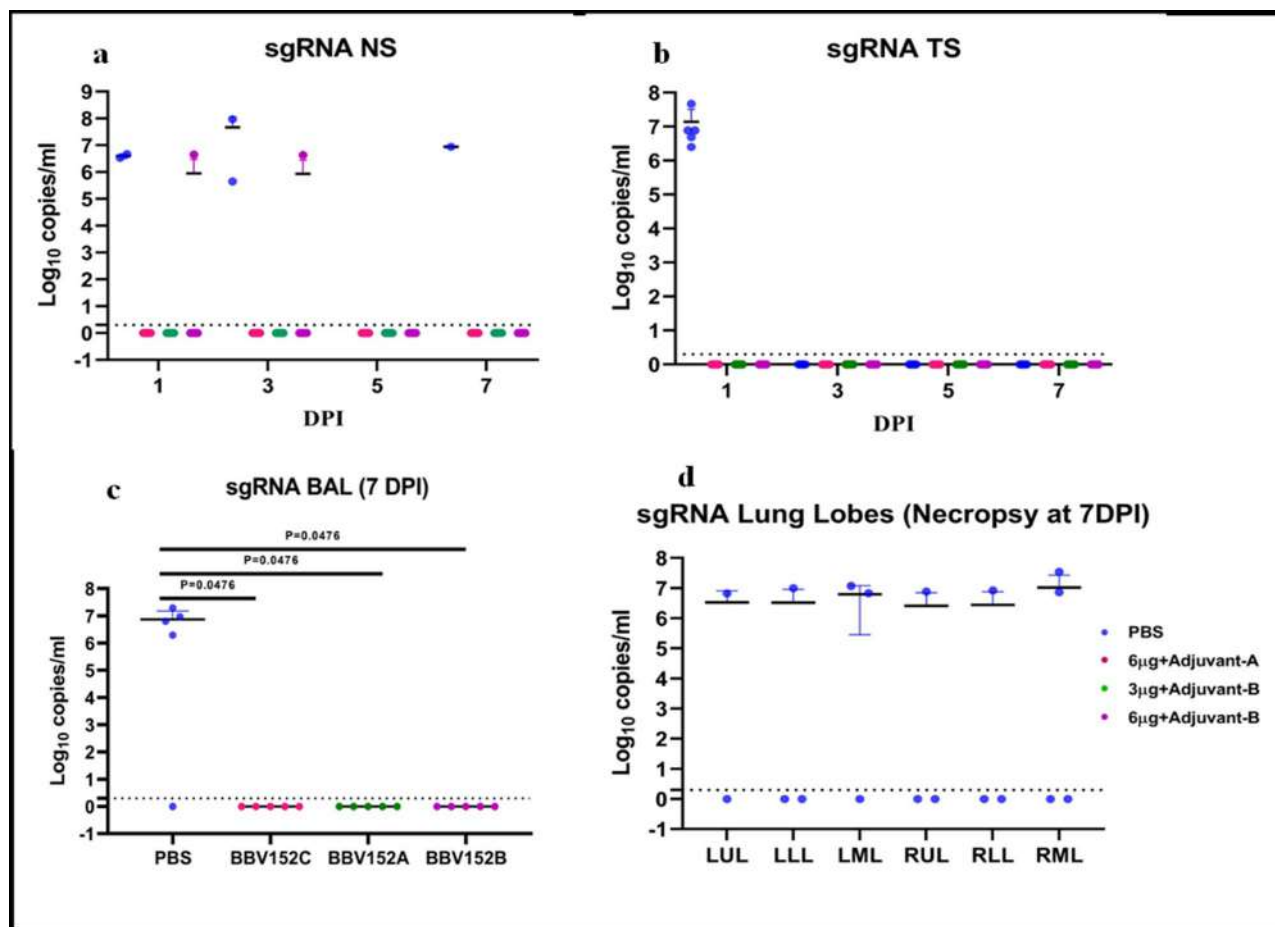


Fig. 4 Subgenomic viral RNA detection in the respiratory tract specimens. sgRNA load in (a) BAL at 7 DPI, (b) sgRNA in different lobes of lungs at 7 DPI, (c) throat swab at 1 DPI and (d) sgRNA load in NS at 1, 3, 5 and 7 DPI. The statistical significance was assessed using the Kruskal-Wallis test followed by the two-tailed Mann-Whitney test between the two groups; P values < 0.05 were considered to be statistically significant. The dotted lines indicate the limit of detection of the assay. Data are presented as mean values \pm standard deviation (SD). Statistical comparison was done by comparing the vaccinated group with the placebo group as a control. Group I = blue, group II = pink, group III = green and group IV = purple, number of animals = 5 animals in each group. Source data are provided as a Source Data file.

procurement of reagents. This fact was a major limiting factor because of which detailed T-cell immunogenicity during vaccination and post-viral challenge period could not be performed. However, in spite of this limitation, the immunogenicity and protective efficacy have been amply demonstrated by the serological response (IgG, NAb), viral clearance from BAL fluid and respiratory tract tissues/organs and necropsy findings in the vaccinated animals compared to the placebo group.

Altogether, this study demonstrates that a two-dose vaccination regimen using 3- μ g dose of the vaccine candidate with adjuvant B induces a significant immune response and provides effective protection in animals challenged with SARS-CoV-2.

Methods

Ethics statement. The study was approved by the Institutional Project Review Committee, and Institutional Biosafety Committee, ICMR-National Institute of Virology (NIV), Pune. The study was recommended by the Institutional Animal Ethics Committee (registration 43/GO/ReBi/SL/99/CPCSEA) and further approved by Committee for the Purpose of Control and Supervision of Experiments on Animals (CPCSEA), New Delhi letter No. V11011 (13)/7/2020-CPCSEA-DADF dated 08.06.2020. The permission from the Office of Principal Chief Conservator of Forests (PCCF), Maharashtra state, was obtained for capturing of 30 rhesus macaques from the wild. A decline in the macaque population was observed in the permitted areas of Maharashtra state, India, due to the habitat change of macaques probably imposed by food scarcity during the COVID-19 lockdown period of India (March 25, 2020 till May 31, 2020). Hence, twenty rhesus macaques (12 male and 8 female) were captured using experienced monkey catchers with the prior approval

from PCCF, Maharashtra state, India. The approximate age of the animals was determined based on the dentition and body measurements. The research was conducted in compliance with the guidelines laid down by CPCSEA, Government of India²³.

Generation of vaccine. Vero CCL-81 cells were initially grown in tissue culture flasks and cell stacks using Dulbecco's Modified Eagle Medium (DMEM) (Sigma-Aldrich, India) containing 10% newborn calf serum (NBCS) (Sigma-Aldrich, India). SARS-CoV-2 strain, NIV-2020-770, (GISAID ID: EPI_ISL_420545) isolated in Vero CCL-81 cells was used for the vaccine development²⁴. The virus strain belongs to the G clade according to the GISAID classification and is 99.97% identical to the Wuhan Hu-1 strain²⁵. G clade sequences are predominantly circulating in India and contribute to ~74% of the SARS-CoV-2 sequences circulating in the world^{26–28}. The genetic stability of the NIV-2020-770 strain was demonstrated by multiple passages in Vero CCL-81 cells and by next-generation sequencing⁷. Virus propagation was done in a bioreactor (Corning Life Science) at the temperature of $36 \pm 1^\circ\text{C}$ and was harvested at 36–72 h post infection and supernatants were collected, clarified and aliquoted. All the infectious work was performed in a biosafety level-3 laboratory. The virus was inactivated with β -propiolactone at a ratio of 1:2500 at $2–8^\circ\text{C}$ for 24–32 h. It was further purified by column chromatography and concentrated using a tangential flow filtration system.

Three formulations of inactivated SARS CoV-2 vaccine candidates were prepared with two adjuvants (A and B): Algel 1 (aluminium hydroxide gel) and Algel 2 (imidazoquinoline, aTLR7/TLR8 agonist adsorbed on aluminium hydroxide gel). In this study, we have defined Algel 1 as Adjuvant A and Algel 2 as adjuvant B. Preliminary immunogenicity and safety study of BBV152 with Algel 1 and Algel 2, in various doses 3, 6 and 9 μ g doses, were performed in mice, rat and rabbit model⁷. Based on the observations of this study, three candidate formulations (6 μ g + Algel 1 (BBV152A), 3 μ g + Algel 2 (BBV152B) and 6 μ g + Algel 2 (BBV152C)) were chosen. Algel 2 was found eliciting high NAb titres and

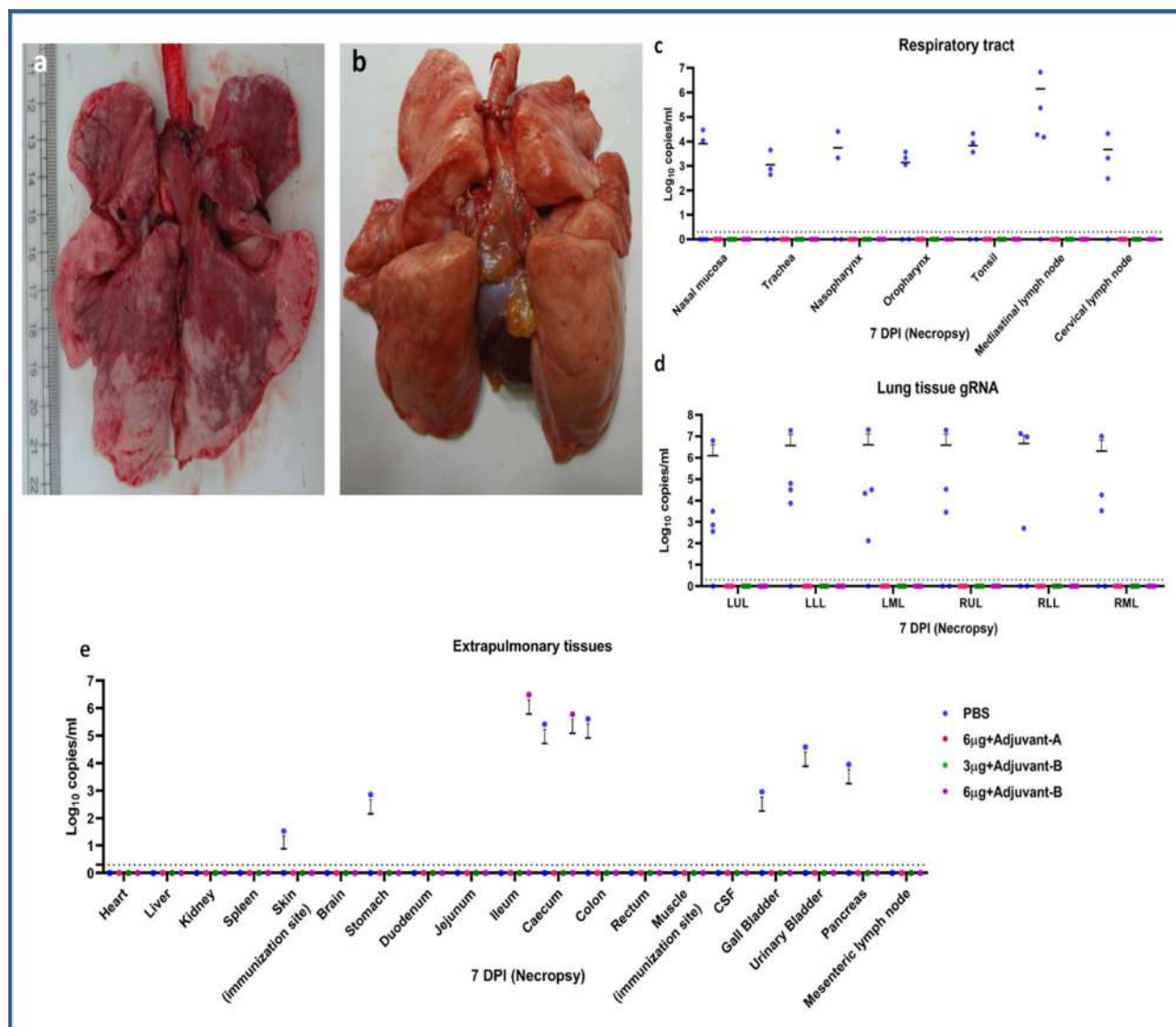


Fig. 5 Gross pathology of lungs and viral RNA load in different tissues. **a** Lungs showing extensive involvement of the right upper lobe (RUL), right lower lobe (RLL), left upper lobe (LUL) and left lower lobe (LLL) (group I) and **(b)** normal lung (group III) **(c)** genomic viral RNA of respiratory tract tissues **(d)**, lungs tissue and **(e)** extrapulmonary organs at 7 DPI. The dotted lines indicate the limit of detection of the assay. Group I = blue, group II = pink, group III = green and group IV = purple, number of animals = 5 animals in each group. Source data are provided as a Source Data file.

robust T-cell immunity. Further, these three candidate formulations were studied for their protective efficacy against SARS-CoV-2 in Syrian hamster model and all the candidates were found immunogenic and protective⁸.

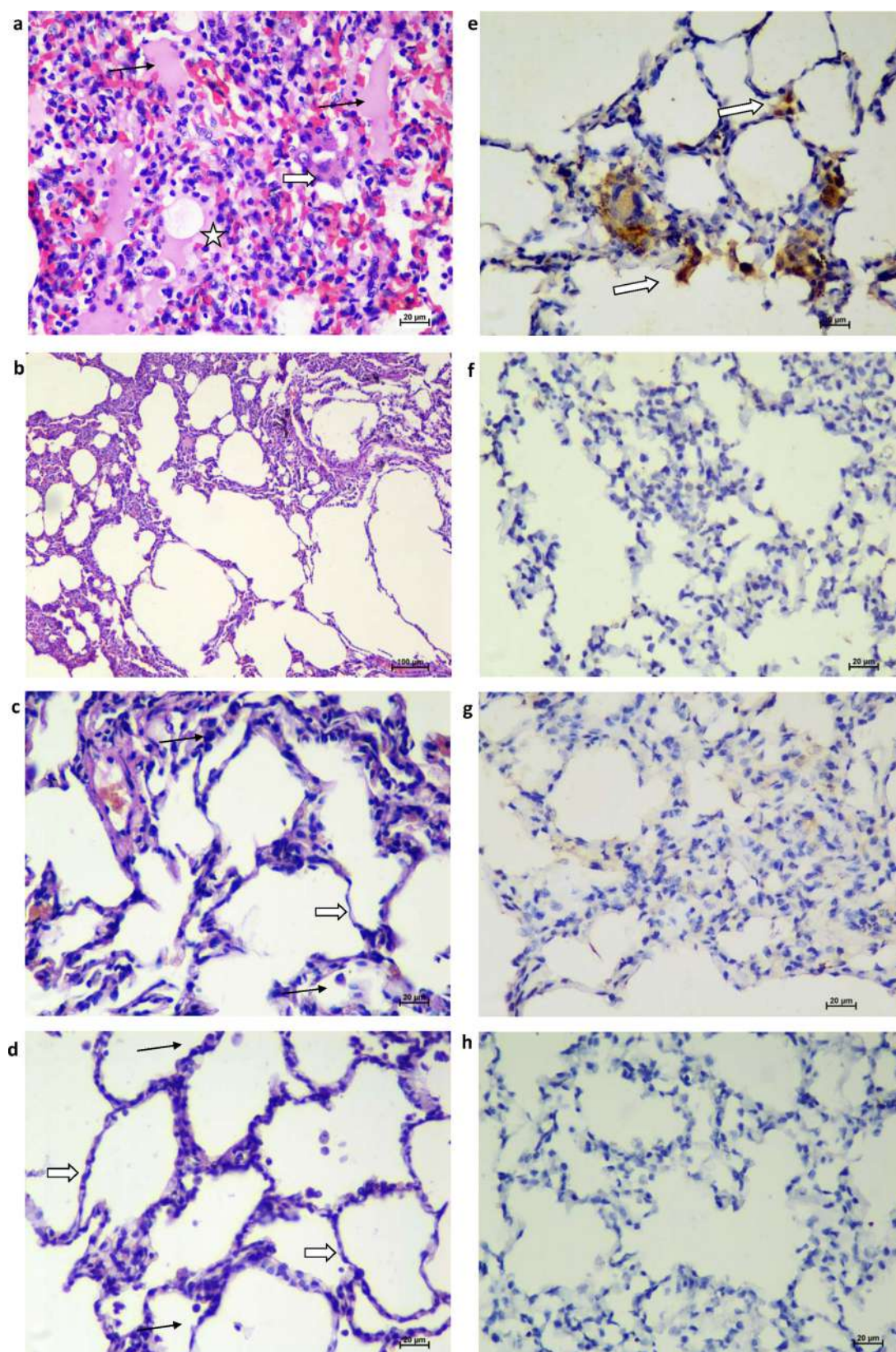
Study design and experiments on rhesus macaques. Rhesus macaques (*Macaca mulatta*) were housed in individual cages at the animal facility of ICMR-NIV, Pune. The animals were maintained on commercial pelleted feed, fruits, vegetables and ad libitum potable drinking water with a 12-h/12-h dark/light cycle. All the animals were clinically evaluated for skin/systemic disorders, haemoglobin, total leukocyte count, differential leukocyte count, platelet count, packed cell volume, biochemical parameters (AST, ALT, bilirubin, serum proteins, alkaline phosphatase, LDH, BUN, creatinine, cholesterol, triglycerides, sodium, potassium and glucose), abdominal ultrasonography, chest X-ray and tuberculin test and were found fit for the study. Animals were screened for Kyasanur forest disease virus and SARS-CoV-2 and IgG antibodies were found to be negative^{29,30}. Biomedical data systems temperature transponder was implanted in the interscapular region subcutaneously for monitoring of body temperature during the study.

Twenty adult animals aged 3–12 years were divided into four groups of five animals (3 M, 2 F) each viz. placebo group, groups II, III and IV. The placebo group was administered phosphate buffer saline (PBS), groups II, III and IV were immunised with formulations of purified inactivated SARS-CoV-2 vaccine candidates: 6 µg + adjuvant-A, 3 µg + adjuvant-B and 6 µg + adjuvant-B, respectively. Animals were administered with two doses of vaccine/placebo on days 0 and 14, respectively, intramuscularly in the deltoid region. Blood samples were

collected on 0, 12, 19, 26 and 28 days for assessing anti-SARS IgG antibody and NAb titres (Fig. 1a).

After completion of 28 days of immunisation, animals were shifted to animal biosafety level-4 facility. Animals were challenged with 1 ml of SARS-CoV-2 (P-3, NIV-2020770, TCID₅₀ 10^{6.5}/ml)²⁴ intratracheally and 0.25 ml in each nostril. Animals were monitored twice daily and clinical scoring was performed based on parameters as listed in Supplementary Table 1. Clinical examination was done on 0, 1, 3, 5 and 7 DPI along with body temperature, body weight, pulse rate and oxygen saturation at room air (Supplementary Table 1). NS, TS, rectal swab (RS), chest X-ray, blood specimens and BAL fluid were collected on 0, 1, 3, 5 and 7 DPI. BAL fluid collection was performed using a flexible paediatric bronchoscope (3.9 mm) (Pentax Medical India Private Limited) under general anaesthesia. The bronchoscope was inserted into the trachea and was guided through bronchus past the third bifurcation; 3–5 ml of saline was instilled at room temperature and aspiration was stopped after we had recovered 30–50% of the instilled volume. The weight of the monkeys in our study varied from 2.5 to 9.5 kilograms and hence installation of larger volumes of saline would have been detrimental to the health of the animals as bronchoscopy was being conducted every alternate day till 7 DPI. On 7 DPI during bronchoscopy prior to necropsy, we instilled a total volume of 10–15 ml of saline for BAL fluid collection.

During necropsy, the following organs: brain, nasal mucosa, tonsil, nasopharynx, oropharynx, cervical lymph node, trachea, lungs, mediastinal lymph node, heart, spleen, liver, kidneys, urinary bladder, gastrointestinal tract, skin along with underlying deltoid muscle from the immunisation site and cerebrospinal fluid (CSF) were collected.



Enzyme-linked immunosorbent assay for detection of anti-SARS-CoV-2 IgG antibody. Immunoplates (Maxisorp, Nun) were coated with 100 μ l/well of SARS-CoV-2 antigen overnight at 4 °C in the carbonate buffer. Subsequently, wells were blocked with liquid plate sealer (CANDOR Bioscience GmbH, Germany) for 2 h at room temperature) 25–30 °C. One-hundred microlitres of diluted rhesus macaque serum sample 1:100 in 1% bovine serum albumin in 1 \times PBS containing 0.1%

Tween (PBST) were added to duplicate wells and incubated at 37 °C for one hour. To each well, 100 μ l of a 1:15000 dilution of goat anti-monkey IgG peroxidase-conjugated antibodies (Sigma, USA) were added and incubated at 37 °C for 1 h. The plates were washed five times with a wash buffer (1 \times PBST) post all incubations. One-hundred microlitres of (3,3',5,5'-Tetramethylbenzidine (TMB) substrate was added and incubated for 10 min. The reaction was stopped by 1N H₂SO₄ and

Fig. 6 Histopathological and immunohistochemical findings. **a** Lungs showing moderate acute inflammatory changes with haemorrhages and infiltration of inflammatory cells. Alveolar septa showed hyaline membrane formation (asterisks) with inflammatory cells and RBCs. The adjacent alveolar interstitium is thickened by oedema (black arrow) and moderate infiltration of lymphocytes, neutrophils and macrophages (white broad arrow). Haematoxylin and eosin-stained (H&E), $\times 400$ magnification. **b** Lungs showing normal histomorphological features of alveolar septa with type I pneumocyte (white arrow) and occasional alveolar macrophages (black arrow) along the alveolar lumen in group II H&E, $\times 400$ magnification. **c** Lung section depicting normal histomorphological features of alveolar septa with type I pneumocyte (white arrow) and occasional alveolar macrophages (black arrow) along the alveolar lumen in group III H&E, $\times 400$ magnification. **d** Lung section depicting normal histomorphological features of alveolar septa with type I pneumocyte (white arrow) and occasional alveolar macrophages (black arrow) along the alveolar lumen in group IV H&E, $\times 400$ magnifications. **e** Lungs section of placebo group showing the presence of viral antigen by immunohistochemistry (IHC) in type-I pneumocytes (arrow) of alveolar septa and in alveolar macrophages (arrow) ($\times 400$ magnification). Lung section of group II (**f**), group III (**g**) and group IV (**h**) showing the absence of viral antigen by IHC. Sixty sections of lung lobe are evaluated for five animals each from groups I, II, III and IV; a representative lesion from each group was selected for the figure.

absorbance was measured at 450 nm³⁰. The sample was considered positive when the P/N ratio was more than 1.5 and optical density (OD) values with the SARS-CoV-2 antigen were above 0.2.

S1-RBD protein-specific SARS-CoV-2 IgG capture ELISA. Anti-SARS-CoV-2 S1 Receptor Binding Domain (RBD) protein IgG in the animal serum was captured by the viral recombinant RBD of S1 subunit of the Spike protein (S1-RBD) coated onto the wells. Serum samples were diluted at the ratio of 1:25, 1:100, 1:400, 1:1600, 1:6400, 1:25,600 and 1:102,400 for titre determination. Fifty microlitres of the diluted samples of each animal at 0 and 7 DPI, positive and negative control, were added to the respective wells. ELISA plate was incubated at 37 °C for 1 h followed by washing with wash buffer five times. Fifty microlitres of ready-to-use anti-monkey IgG HRP was added to each well and was incubated at 37 °C for 30 min. After washing, 100 μ l of liquid TMB substrate added and incubated at room temperature in the dark for 10 min. The reaction was stopped with 100 μ l of stop solution after 10 min. The absorbance was measured at 450 nm. If the OD value of sample tested exceeds 0.2 and sample OD/negative control OD > 2.0, the sample was considered positive.

SARS-CoV-2-recombinant N-protein IgG capture ELISA. Anti-SARS-CoV-2 N protein IgG antibody in the animal serum was detected using recombinant N protein-coated wells. For determination of titre, serum samples were diluted fourfold from 1:25 to 1:102,400. Fifty microlitres of the diluted samples of each animal at 0 and 7 DPI, along with positive and negative control, were added to the respective wells. The ELISA plate was incubated at 37 °C for 1 h. Fifty microlitres of ready-to-use anti-monkey IgG HRP was added and was incubated at 37 °C for 30 min. Plates were washed five times using wash buffer containing 1 \times PBST after each incubation step. One-hundred microlitres of liquid TMB substrate was added and plates were incubated at room temperature in the dark for 10 min. The reaction was stopped with 100 μ l of stop solution. The absorbance was measured at 450 nm. If the OD value of the sample tested exceeds 0.2 and sample OD/negative control OD > 2.0, the sample was considered positive.

Plaque reduction neutralisation test. A fourfold serial dilution of rhesus macaque's serum samples was mixed with an equal amount of virus suspension containing 50–60 plaque-forming units (PFU) in 0.1 ml. After incubating the mixtures at 37 °C for 1 h, each virus-diluted serum sample (0.1 ml) was inoculated onto one well of a 24-well tissue culture plate containing a confluent monolayer of Vero CCL-81 cells. After incubating the plate at 37 °C for 60 min, an overlay medium consisting of 2% carboxymethyl cellulose (CMC) with 2% foetal calf serum (FCS) in 2 \times MEM was added to the cell monolayer, and the plate was further incubated at 37 °C in 5% CO₂ for 5 days. Plates were stained with 1% amido black for an hour. Antibody titre was defined as the highest serum dilution that resulted in >50 (PRNT50) reduction in the number of plaques³¹. The serum samples of each animal were also tested with heterologous virus strain Q-100 and Q-111. Both these strains belong to unclassified clade isolated from COVID-19 positive patient's samples from Iran²⁴.

Detection of SARS-CoV-2 genomic and subgenomic viral RNA. The organs harvested during necropsy were uniformly weighed and homogenised (Tissue homogenizer, Qiagen, Germany) using 1 ml of sterile MEM (GIBCO, Thermo Fisher Scientific, USA). Two-hundred microlitres of each specimen (NS, TS, rectal swab, whole blood, BAL fluid, urine, CSF and tissue homogenates) were used for RNA extraction using MagMAX™ Viral/Pathogen Nucleic Acid Isolation Kit (Thermo Fisher Scientific, USA). SARS-CoV-2 real-time RT-PCR was performed using a 25- μ l reaction containing 5 μ l of RNA, 12.5 μ l of 2 \times reaction buffer provided with the Superscript III one-step RT-PCR system with Platinum Taq Polymerase (Invitrogen, Darmstadt, Germany), 1 μ l of reverse transcriptase/Taq mixture from the kit, 1.5 μ l of Primer and probe mix (Supplementary Table 4). Thermal cycling was performed at 55 °C for 30 min for reverse transcription, followed by 95 °C for 3 min and then 45 cycles of 95 °C for 15 s, 58 °C for 30 s. A

standard curve was plotted using serially diluted tenfold (10^1 – 10^{10}) in vitro-transcribed RNA for E gene (gRNA)^{32,33}. E sgRNA was amplified using real-time RT-PCR from the above specimens using primers as shown in Supplementary Table 4. Thermal cycling was performed at the same cycling conditions as mentioned for E gene. A standard curve was plotted using serially diluted tenfold (10^1 – 10^{10}) in vitro-transcribed E sgRNA³⁴.

Lymphocyte subset and cytokine/chemokine profile. To analyse phenotype and proportion of T helper, T cytotoxic and B cells, anti-coagulated (0.1 ml) whole blood was surface-stained with appropriate fluorochrome-conjugated antibodies along with their corresponding isotype controls. Two sets of sample tubes were prepared, one for T cell (CD3-FITC, CD8-PE and CD4-APC) and another for B cell (CD45-PerCP, CD3-FITC and CD20-PE). After incubation for 30 min at 4 °C in the dark, 2 ml of RBC lysing buffer were added to each tube, vortexed and incubated at room temperature for 12 min. Two millilitres of washing solution was added to each tube. The sample tubes were centrifuged at 200 \times g for 5 min, and the supernatant was carefully aspirated out. The cell pellets were suspended in 500 μ l of wash buffer and vortexed. The levels of IL-2, IL-5, IL-6, IL-8, IFN- γ and TNF- α in the serum samples were analysed using BD cytometric bead array flex sets, as per the manufacturer's instructions³⁵. Cytokine levels were measured on a BD FACSCalibur™ flow cytometry (BD Biosciences) using BD CellQuest™ Pro software V5.1. The data were analysed using flow cytometric analysis program (FCAP) Array™ software V3. The detection sensitivities of IL-2, IL-5, IL-6, IL-8, IFN- γ and TNF- α were 11.2, 1.1, 1.6, 1.2, 1.8 and 1.2 pg/ml, respectively.

Virus isolation from clinical/necropsy specimens. One-hundred microlitres of each specimen was inoculated onto 24-well Vero CCL-81 cell monolayers maintained in MEM (Gibco, UK) and incubated for 1 h at 37 °C with rocking every 10 min. Subsequently, media was removed and cells were washed with 1 \times PBS. Media with 2% FBS was added to each well and was incubated in a CO₂ incubator at 37 °C for 5 days. The culture plate was examined daily for CPE using an inverted microscope (Nikon, Eclipse Ti, Japan). The cell culture supernatant from the wells showing CPE was further confirmed by real-time RT-PCR²⁴.

Histopathological examination and immunohistochemistry. Histopathological evaluation of all the six lobes of lungs of animals was performed on 7 DPI after necropsy. Tissue sections from lungs were immersion-fixed in 10% neutral buffered formalin. The fixed tissues were processed using an automated tissue processor using alcohol-xylene protocol for dehydration and clearing. The processed tissues were embedded in paraffin and were sectioned to 4–5 μ m-thick sections using an automated microtome (Leica, Germany). The cut tissue sections were stained by haematoxylin and eosin³⁶. The factors considered and reporting criteria used were as per the recommendation of the Working Group of the Society of Toxicologic Pathology's Scientific and Regulatory Policy Committee³⁷. Seven parameters were assessed during the histopathological examination of slides for lung sections in all animals for assessing the severity of disease in the lungs as mentioned in Supplementary Table 2. The parameters listed in Supplementary Table 2 were graded as no abnormality detected (NAD), minimal (+1), mild (+2), moderate (+3) or severe (+4) for each lung. Subsequently, the extent of disease for each lobe of animals was opined upon as mild, moderate and severe. Further, the analysis was done on the severity of infection depending on the number of lobes having evidence of disease for animals of placebo and vaccinated groups. Anti-SARS-CoV-2 immunoreactivity in the lung tissues was assessed using mouse polyclonal serum. For IHC, mouse polyclonal serum was used as the primary antibody (1:500) and anti-mouse HRP antibody was used as secondary antibody^{29,36}.

Statistical analysis. Clinical, virological, haematological, biochemical and immunological data were analysed using GraphPad Prism software version 8.4.3 (GraphPad, San Diego, California) and Stata software version 14. (StataCorp LLC, USA). The clinical, virological and serological data for the different groups were initially compared using the nonparametric Kruskal–Wallis test. The groups that

were significant using the Kruskal–Wallis test were further assessed using the Mann–Whitney test. A group-wise comparison was performed to assess significance between the placebo and the other vaccinated groups using a two-tailed Mann–Whitney test. The P values < 0.05 were considered significant and are marked on the figures. Nonsignificant values are not depicted in the figures. The log10 plots below the detection limits are depicted as 1 for the illustration purpose. The detection limits are marked with the dotted lines on the respective figures.

Reporting summary. Nature research reporting summary linked to this paper contains the information on research design. Further information on research design is available in the Nature Research Reporting Summary linked to this article.

Data availability

Data are available in the paper and in the Supplementary Material. All other relevant data are available from the authors. Source data are provided with this paper.

Received: 28 August 2020; Accepted: 4 February 2021;

Published online: 02 March 2021

References

- Wang, C. et al. A novel coronavirus outbreak of global health concern. *Lancet* **395**, 470–473 (2020).
- World Health Organization. WHO coronavirus disease (COVID-19) dashboard. <https://covid19.who.int/> (2020).
- World Health Organization. Module 2: types of vaccine and adverse reactions. https://www.who.int/vaccine_safety/initiative/tech_support/Part-2.pdf (2020).
- Krammer, F. SARS-CoV-2 vaccines in development. *Nature* **586**, 516–527 (2020).
- Wang, H. et al. Development of an inactivated vaccine candidate, BBIBP-CoV, with potent protection against SARS-CoV-2. *Cell* <https://doi.org/10.1016/j.cell.2020.06.008> (2020).
- Gao, Q. et al. Development of an inactivated vaccine candidate for SARS-CoV-2. *Science* <https://doi.org/10.1126/science.abc1932> (2020).
- Ganneru, B. et al. Evaluation of safety and immunogenicity of an adjuvanted, TH-1 skewed, whole virion inactivated SARS-CoV-2 vaccine-BBV152. Preprint at <https://www.biorxiv.org/content/10.1101/2020.09.09.285445v1> (2020).
- Mohandas, S. et al. Immunogenicity and protective efficacy of BBV152: a whole virion inactivated SARS-CoV-2 vaccine in the Syrian hamster model. *iScience* 102054 <https://doi.org/10.1016/j.isci.2021.102054> (2021).
- Doremalen, N. et al. ChAdOx1 nCoV-19 vaccine prevents SARS-CoV-2 pneumonia in rhesus macaques. *Nature* **30**, 1–8 (2020).
- Mercado, N. B. et al. Single-shot Ad26 vaccine protects against SARS-CoV-2 in rhesus macaques. *Nature* **30**, 1–1 (2020).
- Corbett, K. S. et al. Evaluation of the mRNA-1273 Vaccine against SARS-CoV-2 in nonhuman primates. *N. Engl. J. Med.* <https://doi.org/10.1056/NEJMoa2024671> (2020).
- Patel, A. et al. Intradermal-delivered DNA vaccine provides anamnestic protection in a rhesus macaque SARS-CoV-2 challenge model. Preprint at <https://www.biorxiv.org/content/10.1101/2020.07.28.225649v1> (2020).
- Annette, B. et al. A prefusion SARS-CoV-2 spike RNA vaccine is highly immunogenic and prevents lung infection in non-human primates. Preprint at <https://www.biorxiv.org/content/10.1101/2020.09.08.280818v1> (2020).
- US Food and Drug Administration. Pfizer-BioNTech COVID-19 vaccine. <https://www.fda.gov/emergency-preparedness-and-response/coronavirus-disease-2019-covid-19/pfizer-biontech-covid-19-vaccine> (2021).
- Speranza, E. et al. SARS-CoV-2 infection dynamics in lungs of African green monkeys. *Cell* (2020).
- Alexandersen, S. et al. SARS-CoV-2 genomic and subgenomic RNAs in diagnostic samples are not an indicator of active replication. *Nat. Commun.* **11**, 6059 (2020).
- Yang, X. et al. Clinical course and outcomes of critically ill patients with SARS-CoV-2 pneumonia in Wuhan, China: a single-centered, retrospective, observational study. *Lancet. Respir. Med.* **8**, 475–481 (2020).
- Mazzoni, A. et al. Impaired immune cell cytotoxicity in severe COVID-19 is IL-6 dependent. *J. Clin. Invest.* <https://doi.org/10.1172/JCI138554> (2020).
- Chen, Z. & John Wherry, E. T cell responses in patients with COVID-19. *Nat. Rev. Immunol.* 1–8. <https://doi.org/10.1038/s41577-020-0402-6> (2020).
- Chandrasekar, A. et al. SARS-CoV-2 infection protects against rechallenge in rhesus macaques. *Science* **80**, 4776 (2020).
- Surh, C. D. & Sprent, J. Homeostasis of naive and memory T cells. *Immunity* **29**, 848–862 (2008).
- Lindsley, A. W. et al. Eosinophil responses during COVID-19 infections and coronavirus vaccination. *J. Allergy Clin. Immunol.* **146**, 1–7 (2020).
- Committee for the Purpose of Control and Supervision on Experiments on Animals. CPCSEA guidelines for laboratory animal facility. *Indian J. Pharmacol.* **35** <https://doi.org/10.13140/2.1.3877.2802> (2020).
- Sarkale, P. et al. First isolation of SARS-CoV-2 from clinical samples in India. *Indian J. Med. Res.* **151**, 244–250 (2020).
- Potdar, V. et al. Genomic analysis of SARS-CoV-2 strains among Indians returning from Italy, Iran & China, & Italian tourists in India. *Indian J. Med. Res.* **151**, 255–260 (2020).
- Kumar, N. et al. Distribution of the genetic clade “G” of SARS-CoV-2—an insight into COVID-19 virulence and spread in India. <https://doi.org/10.35543/osf.io/5fzup> (2020).
- Hadfield, J. et al. Nextstrain: real-time tracking of pathogen evolution. *Bioinformatics* **34**, 4121–4123 (2018).
- Mercatelli, D. et al. Geographic and genomic distribution of SARS-CoV-2 mutations. *Front. Microbiol.* **11**, 1800 (2020).
- Patil, D. R. et al. Study of Kyasanur forest disease viremia, antibody kinetics, and virus infection in target organs of *Macaca radiata*. *Sci. Rep.* **10**, 1–3 (2020).
- Sapkal, G. et al. Development of indigenous IgG ELISA for the detection of anti-SARS-CoV-2 IgG. *Indian J. Med. Res.* **151**, 444–449 (2020).
- Perera, R. A. et al. Serological assays for severe acute respiratory syndrome coronavirus 2 (SARS-CoV-2). *Eur. Surveill.* **25**, 2000421 (2020).
- Choudhary, M. L. et al. Development of in vitro transcribed RNA as positive control for laboratory diagnosis of SARS-CoV-2 in India. *Indian J. Med. Res.* **151**, 251–254 (2020).
- World Health Organization. *Coronavirus Disease (COVID-19) Technical Guidance: Laboratory Testing for 2019-nCoV in Humans*. <https://www.who.int/emergencies/diseases/novel-coronavirus-2019/technical-guidance/laboratory-guidance> (WHO, 2020).
- Wölfel, R. et al. Virological assessment of hospitalized patients with COVID-2019. *Nature* **581**, 465–469 (2020).
- Kaushal, H. et al. Evaluation of cellular immunological responses in mono- and polymorphic clinical forms of post-kala-azar dermal leishmaniasis in India. *Clin. Exp. Immunol.* **185**, 50–60 (2016).
- Culling, C. F. A. *Handbook of Histopathological and Histochemical Techniques: Including Museum Techniques* (Butterworth-Heinemann, 2013).
- Schafer, K. A. et al. Use of severity grades to characterize histopathologic changes. *Toxicol. Pathol.* **46**, 256–265 (2018).

Acknowledgements

Authors acknowledge the support and co-ordination from Principal Chief Conservator of Forests (Wildlife), Chief Wildlife Warden, Maharashtra state and Chief Conservator of Forests (Wildlife/Territorial), Pune Forest Division for the experimentation. Authors also acknowledge the support from Deepika Chawdhary, Mayur Mohite, Vishal Gaikwad (Engineering support), Santosh Jadhav and laboratory team that includes Ganesh Chopade, Manjunath Holleppanavar, Rajen Lakra, Darpan Phagiwal, Chetan Patil, Chandrakant Upadhyay, Sanjay Thorat, Ratan More, Madhav Acharya, Malvika Salave, Ashwini Bagmare, Ciyona, Sapna Gawande, Poonam Bodke and Nitin Deshpande. Authors also express gratitude towards the technical team of the animal house, which includes Ankayya Thimnapally, Vitthal Sasane, Sunny K. Athwal, Nikhil Chavan and Swagat Deshkar. We acknowledge the generous support of Dr. Kavita Lole, Group Leader and Scientist F, Hepatitis division, ICMR-NIV, Pune, for sharing the in-vitro-transcribed RNA required to determine sgRNA copy number. We sincerely acknowledge Major General Arindam Chatterjee, Commandant, AICTS, Pune, Major General S. Hasnain, Commandant, Command Hospital (Southern Command) Pune, India and Dr. Smita Mahale, Director, ICMR-National Institute for Research in Reproductive Health, Mumbai, India for extending generous support for the study. We would also thank Havaladar Mangesh Aamre, AICTS, Pune for his excellent support in bronchoscopy.

Author contributions

P.D.Y., K.M.E., K.M., P.A., N.G. and B.B. conceived and designed the study. K.M.E., K.M., R.E., V.K.S., S.D.P. and B.S. performed vaccine design and production. P.D.Y., S.K., S.L.M. and D.R.P. performed the planning of the animal experiment. S.K., D.R.P., S.L.M., G.B., K.A., S.M.M., B.M. and M.D.G. performed the animal experimentation. P.D.Y., A.M.S., G.S., H.K., D.N., R.J., G.D. and D.Y.P. performed the laboratory work planning and data analysis. A.M.S., P.D.Y. and R.J. developed the in-house ELISA. G.D., C.M., H.K., S.P., R.J., A.N.K., Y.J., T.M., P.S., S.B., D.M., K.K., S.S., R.G., P.G. and H.D. performed sample processing in the laboratory. S.F., A.S., M.K., A.K., S.D. and S.G. assisted in animal experimentation. P.D.Y., S.K., A.M.S., D.Y.P. and S.L.M. have drafted the paper. P.D.Y., A.S.A., D.Y.P., S.K., P.A., N.G., S.M.P., R.R.G. and B.B. substantively revised it. All authors reviewed the paper and agree to its contents.

Competing interests

The authors declare no competing interests.

Additional information

Supplementary information The online version contains supplementary material available at <https://doi.org/10.1038/s41467-021-21639-w>.

Correspondence and requests for materials should be addressed to B.B.

Peer review information *Nature Communications* thanks Ronald Veazey and the other, anonymous, reviewer(s) for their contribution to the peer review of this work.

Reprints and permission information is available at <http://www.nature.com/reprints>

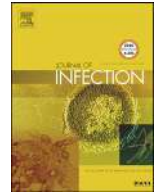
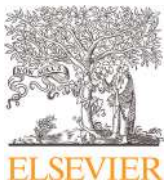
Publisher's note Springer Nature remains neutral with regard to jurisdictional claims in published maps and institutional affiliations.



Open Access This article is licensed under a Creative Commons Attribution 4.0 International License, which permits use, sharing, adaptation, distribution and reproduction in any medium or format, as long as you give appropriate credit to the original author(s) and the source, provide a link to the Creative Commons license, and indicate if changes were made. The images or other third party material in this article are included in the article's Creative Commons license, unless indicated otherwise in a credit line to the material. If material is not included in the article's Creative Commons license and your intended use is not permitted by statutory regulation or exceeds the permitted use, you will need to obtain permission directly from the copyright holder. To view a copy of this license, visit <http://creativecommons.org/licenses/by/4.0/>.

© The Author(s) 2021

¹Indian Council of Medical Research-National Institute of Virology, Pune 411021 Maharashtra, India. ²Bharat Biotech International Limited, Genome Valley, Hyderabad 500 078 Telangana, India. ³Department of Neurosurgery, Command Hospital (Southern Command), Armed Forces Medical College (AFMC), Pune 411040 Maharashtra, India. ⁴Army Institute of Cardio-Thoracic Sciences, Pune 411040 Maharashtra, India. ⁵Indian Council of Medical Research, V. Ramalingaswami Bhawan, New Delhi 110029, India. ⁶ICMR-National Institute for Research in Reproductive Health, Mumbai 400012 Maharashtra, India. ⁷Department of Veterinary Pathology, Krantisinh Nana Patil College of Veterinary Science, Shirwal 412801 Maharashtra, India. ✉email: balrambargava@yahoo.com



Letter to Editor

First two cases of Monkeypox virus infection in travellers returned from UAE to India, July 2022

Dear Editor,

Recently, Orviz *et al.*, reported the clinical and virological aspects of Monkeypox cases in Spain during May–June 2022.¹ Since 1970, the Monkeypox virus (MPXV), belonging to *Orthopoxvirus* genus and *Poxviridae* family, has been endemic in Central and West Africa.² It has now have shown the emergence in various non-endemic countries in 2022 due to the importation from endemic countries due to further community transmission.³ On 23 July the World Health Organization declared Public Health Emergency of International Concern considering the global monkeypox outbreaks all the six regions affecting multiple countries. The West African and Central Africa (Congo Basin) are the two known clades of the MPXV. The Congo Basin strain causes more severe illness, 0–11% mortality and increased transmissibility.⁴ The West African clade is been circulating in the ongoing 2022 outbreaks.⁵

Here, we report the detection and genomic characterization of first two MPXV cases travelled from United Arab Emirates (UAE) to India during July 2022.

Case 1, a 35-year, male, engineer and resident of UAE had developed low-grade fever and myalgia on 5 July 2022. On the next

day, he developed multiple vesicular rashes in the oral cavity and lips followed by single lesion on the genital organ [Fig. 1A]. The lesions were umbilicated with the size 0.5 to 0.8 cm. Subsequently, the upper lip became oedematous and then he developed umbilicated vesicular lesions in right infra-mammary, right-tragus, right-temple, and right-deltoid region [Fig. 1B]. He also had maculopapular rashes on both hands. With these complaints, he visited a medical facility on 9 and 11 July 2022 [Fig. 1A]. Upon consultation, he revealed history of similar lesions amongst his friends and contact with suspected Monkeypox cases (denied sexual contact), a week prior to onset of symptoms. The clinician had advised the screening for MPXV and prescribed tablet Acyclovir.

However, he travelled from UAE to his hometown Kerala on 12 July 2022. On his return, he developed sore throat with worsening of oral lesions for which he visited a hospital in Kerala. Considering his history of contact with suspected Monkeypox case and pustular lesions, he was referred immediately to Government Medical College Thiruvananthapuram [GMCT] [Fig. 1A]. The patient had no known comorbidities but gave history of self-limiting genital lesions eighteen months ago. During clinical evaluation, multiple cervical and inguinal lymph nodes were palpable, which raised a high suspicion of MPXV infection. The initial hematological and biochemical profile on the same day showed haemoglobin-14.1 gm%,

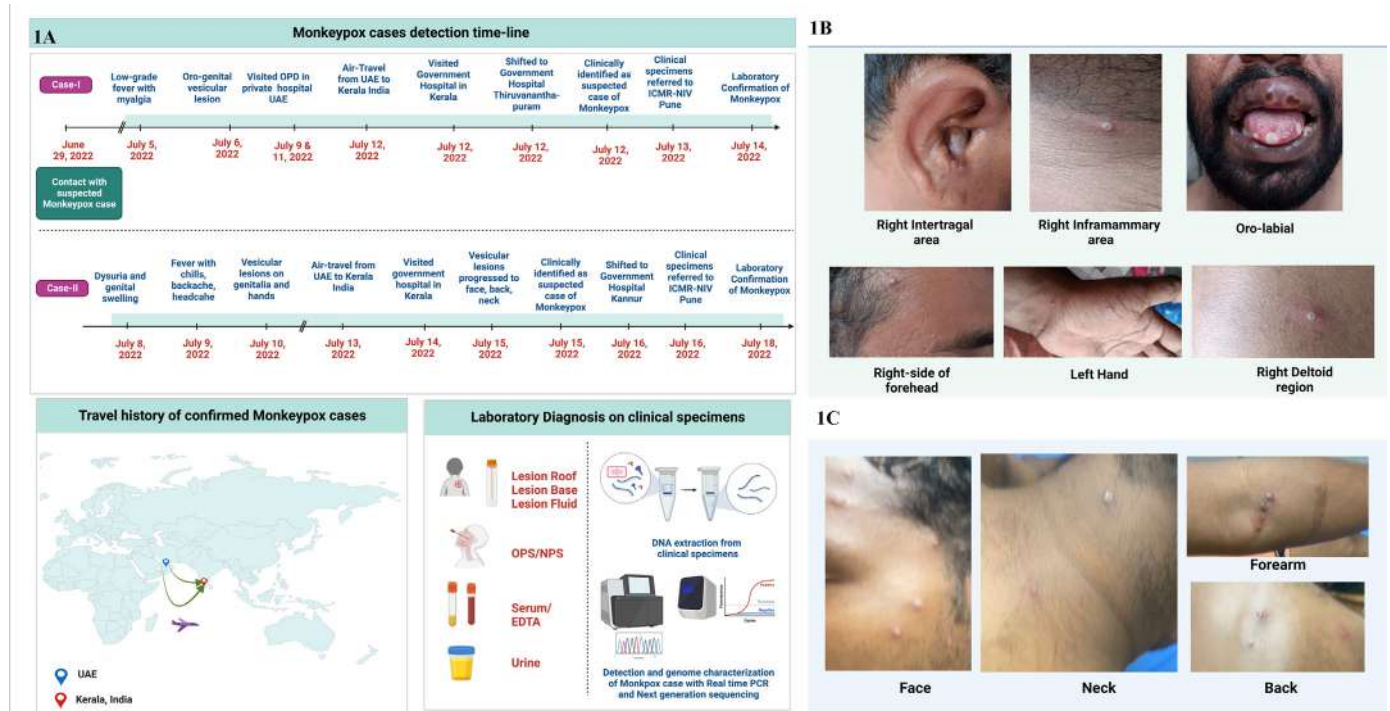


Fig. 1. A–C: A) Graphical presentation depicting the time line of detection, travel history and laboratory diagnosis of first two cases of Monkeypox in India; Umbilicated characteristic MPXV pustular lesions on 9th post onset day of illness of B) Case-I; C) Case-II

leucocytosis [14,600/L], platelets-2,29,000/ μ L and random blood sugar level of 100 mg/dl. Investigations for HSV-1/2, Syphilis and HIV were negative.

Case 2, a 31-year, male, from UAE had developed dysuria and genital swelling on 8 July 2022. On the next day, he developed fever with chills, myalgia, backache and headache. Subsequently, he developed multiple vesicular rashes on the genital organ and on both hands on 10 July 2022. [Fig. 1B]. He travelled from UAE to his hometown in Kerala on 13 July 2022. The lesions progressed and later spread to face, back, neck and forearm with

cervical lymphadenopathy by 15 July 2022 [Fig. 1C]. He visited government hospital locally, he was isolated on 16 July 2022 [Fig. 1A]. He did not have any co-morbidity and denied any sexual or physical contact with suspected or confirmed MPXV case.

The oropharyngeal (OPS) & nasopharyngeal swab (NPS), EDTA blood, serum, urine, lesion samples from multiple sites (lesion fluid, lesion roof and lesion base) of both the cases were collected on ninth post onset day of infection i.e. 13 and 16 July 2022 respectively.

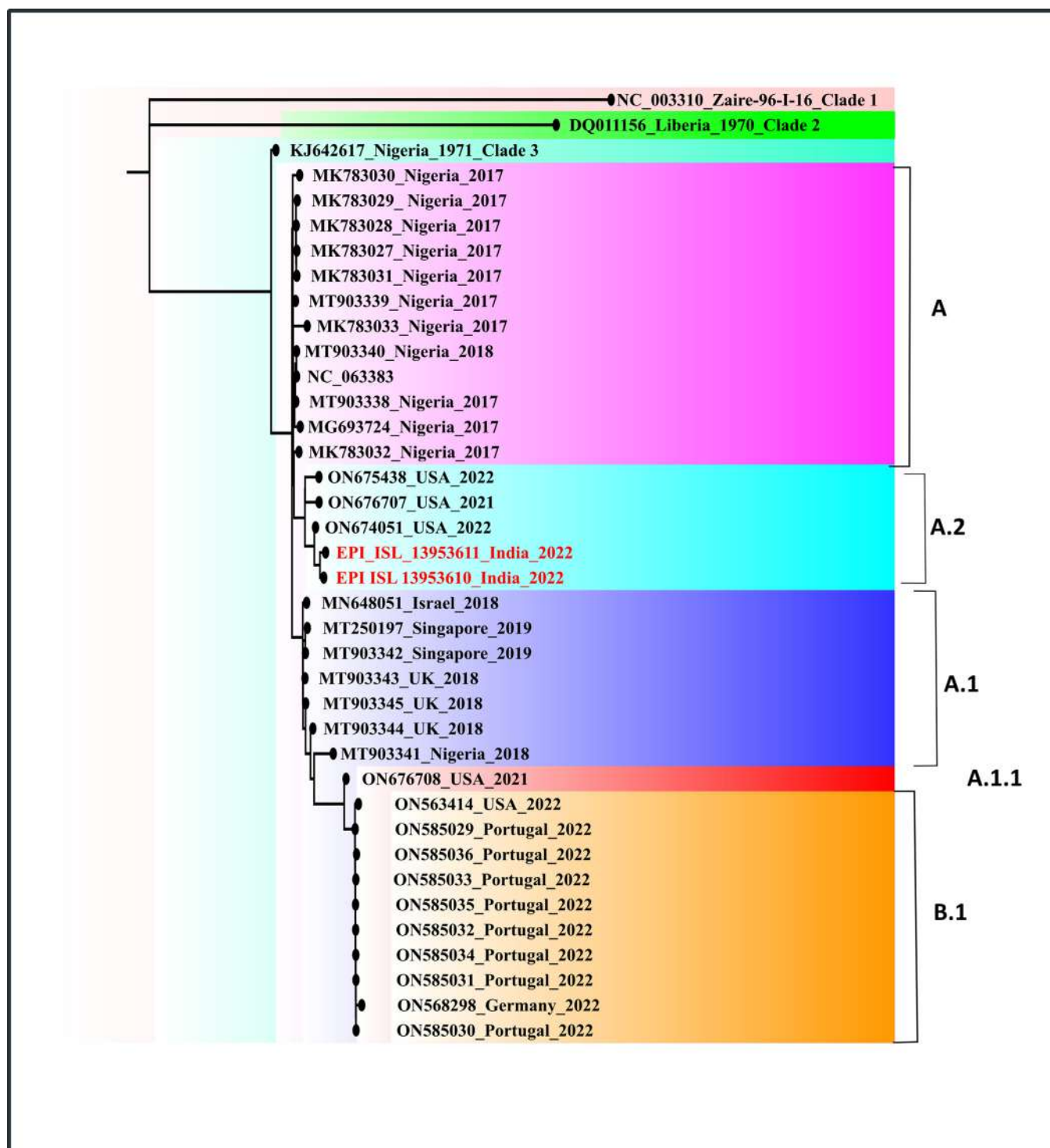


Fig. 2. The phylogenetic tree was constructed using Maximum likelihood method. The reference sequences for the MPXV genome clades and lineages were downloaded from the NCBI website. The MPXV genome sequences retrieved from two confirmed Monkeypox cases in India are marked in red color with GISAID accession ID (EPI_ISL_13953611 and EPI_ISL_13953610) in A.2 lineage along with sequences from USA.

Further, they were referred to the World Health Organization Collaborating Centre for emerging and re-emerging diseases, ICMR-National Institute of Virology, Pune, India for the MPXV diagnosis.

The laboratory diagnosis on the clinical samples of both the cases (OPS, NPS, EDTA blood, serum, urine, lesion fluid, lesion roof and lesion base) was carried out using real time PCR for *Orthopoxvirus*, MPXV, West African clade specific MPXV.^{6,7} All the clinical samples of two cases were positive for MPXV, except the EDTA blood and serum of case 2. The clinical specimens of case 1 showed viral load (Copy number/ml) in the NPS (7.4×10^5 /ml), OPS (3.4×10^6 /ml), urine (3.4×10^6 /ml), serum (1.8×10^6 /ml), EDTA blood (6.8×10^4 /ml), lesion roof (1.1×10^8 /ml), lesion fluid (6.3×10^6 /ml) and lesion base (2.3×10^8 /ml). Similarly for the clinical specimens of case 2 had the viral DNA copy number/ml in NPS/OPS (5.9×10^7 /ml), urine (3.4×10^6 /ml), lesion roof (8.4×10^8 /ml), lesion fluid (2.1×10^7 /ml) and lesion base (5.5×10^8 /ml).

Further, the skin lesions of both the cases were sequenced with next generation sequencing using Illumina platform.⁸ The complete MPXV genome was retrieved from both the cases and analyzed using CLC Genomic Workbench 22.0. The Maximum likelihood tree has been generated in IQ-TREE software with 1000 bootstrap replications. The sequence analysis of case 1 and case 2 revealed similarity of 99.91% and 99.96% respectively with Monkeypox virus isolate MPXV_USA_2022_FL001, complete genome [GenBank accession no. ON674051]. The retrieved sequences [GenBank accession no. EPI_ISL_13953611 and EPI_ISL_13953610] from the clinical specimens of confirmed Monkeypox cases in India belonged to the A.2 lineage of West African clade. Fig. 2. It has significant 34472 nucleotide mutation of allele T. (<https://github.com/nextstrain/monkeypox/blob/master/config/clades.tsv>).

The two close contacts [mother and brother] of the case-1 showed symptoms of sore throat, were screened negative for the MPXV. Considering the surge in COVID-19, cases globally and in India, these cases were screened and brother of the case-patient was found positive for SARS-CoV-2. The three close contacts of case 2 were asymptomatic in observation period.

Recently, the World Health Organization has proposed novel classification for the MPXV genome, where the former Congo Basin (Central African) clade designated as Clade one (I) and West African clade as Clade two (II) with two sub-clades IIa and IIb. All MPXV genomes from the 2022 outbreak belong to West African clade.⁹ The clinico-epidemiological history and laboratory analysis of two confirmed Monkeypox cases in India suggest travel-associated introduction of MPXV infection in the country. The genome of both the cases matched closely with the A.2 lineage. Recently, Gigante et al., demonstrated highest similarity of two MPXV sequences from 2022 outbreak in USA (USA_2022_FL001 and USA_2022_VA001) with MPXV sequences from a 2021 (ON676707), a travel-associated case from Nigeria to Texas which belongs to lineage A.2. The current Monkeypox outbreak in USA represents the circulation of MPXV lineage A.2 from 2021 which has evolved from lineage A that caused the Nigeria outbreak in 2017–2018.¹⁰ The MPXV genome retrieved from confirmed Monkeypox cases with travel history from UAE to India also demonstrated the circulation of A.2 lineage in UAE. Unfortunately, no epidemiological data is available for the introduction of MPXV to UAE. An increase in the number of Monkeypox cases with low mortality rate has been observed with B.1. Its estimated time of emergence in the European continent has been predicted to have occurred in as early as March 2022. The B.1 lineage has significant 77383 nucleotide mutation of allele A.¹¹ However, there is no information available which can differentiate between the transmission pattern of A.2 and B.1 lineage. Since the detection of Monkeypox cases in India, the containment measures have been taken by public health department. This includes the isolation of case and contacts, quick screening of all the symptomatic contacts, strict adherence to the

personal protective equipment and hand hygiene, hospital infection control practices and intense health education in the community. India has demonstrated quick and continuous vigilance and preparedness to detect the first two MPXV cases within a day of entry of the case in the country. This emphasized the alertness of the all stakeholders including airport authority and the clinicians to be alert for the patients who have rash like illness with international travel irrespective of age, gender or sexual orientation. The surveillance of suspected Monkeypox cases could be strengthened by screening the at-risk population such as men who have sex with men (MSM) and female sex workers (FSW) by National AIDS Control Organization, India. Besides this, adhering to the COVID-19 protocol during the air travel would be beneficial for reducing the transmission amongst the co-passengers and crews through respiratory droplets.

Ethical approval

The study was approved by the Institutional Human Ethics Committee of ICMR-NIV, Pune, India under the project 'Providing diagnostic support for referred samples of viral hemorrhagic fever and other unknown etiology and outbreak investigation'. The written informed consents were obtained from both the cases.

Author Contributions

PDY, RRS contributed to study design, data analysis, interpretation and writing and critical review. ARS, SK, AMS, AR, PVK, RB, SSM, SM, DYP, AK, AEG, RR, MS, AU, GNS, MR, SS, PJ, SMJ contributed to data collection, interpretation, writing and critical review. PDY, RRS, ARS, AMS, DYP, PA, NG, NV contributed to the critical review and finalization of the paper.

Financial support & sponsorship

The grant was provided from ICMR-National Institute of Virology, Pune for conducting this study.

Conflicts of Interest

Authors do not have a conflict of interest among themselves.

Acknowledgement

Authors extend gratitude to Smt. Veena George [Hon'ble Minister for Health and Family Welfare, Kerala], for her exemplary leadership and efficient coordination of the Monkeypox virus disease control activities, and "The Team Kerala Health," the district administration, press, media, and people for their efforts in streamlining the public health responses. We would also extend our gratitude towards Mrs. Tinku Biswal, Principal secretary for Health Kerala and Dr. Asha Thomas, Additional Chief secretary Medical Education. The author also extend gratitude to Dr. Thomas Mathew Director of Medical Education; Dr. Preetha PP Director of Health services; Dr. Kala Kesavan P, Principal, Government Medical college Thiruvananthapuram [GMCT]; Dr. Nizarudeen A, Medical superintendent GMCT; Dr. Prathap Somanath, Principal, Government Medical College Kannur; and Dr. Meenakshi V State Surveillance Officer, Additional director of public Health, and Dr. Sandhya, District Surveillance Officer, Kollam for their immense support. The authors are thankful to Dr. Venugol M, Professor and Head of ENT; and Dr. Anil Kumar TV, Professor and Head of Psychiatry GMCT; Dr. Kirankumar VS and Dr. Athul Gurudas Assistant Professors of Infectious diseases at GMCT for their role in patient care. Dr. Aiswarya Babu Heera Junior resident dermatology; Dr. Praveen RK, Junior resident Internal Medicine; Dr. Teny George

Pallipadan and Dr. Ajithalekshmi A S, Junior residents of community medicine GMCT for being part of the treatment team. The authors are thankful to Dr. Anuja M, Associate professor and all members of State Prevention of epidemic and infectious diseases cell for their role in contact tracing. The authors are thankful to Mrs. Sabitha T.S, Chief Nursing officer GMCT and entire nursing and infection control team for their role in treatment of the patient. Authors are thankful to Miss. Vidya M, Research assistant VRDL, GMCT; Miss Annie CS VRDL GMCT and Mr Avin VA, Lab Technician VRDL GMCT for their help in transporting and packing the samples collected. Authors acknowledge Dr. Ajay Krishnan MD, Consultant dermatologist at N.S. Memorial Institute of Medical sciences Kollam for initially suspecting monkeypox and for timely referral to GMCT. The authors are thankful to Prof. Balram Bhargava, Former Secretary Department of Health Research and Director General, ICMR for his encouragement and support. Authors are also thankful to the staff of the Administration section, ICMR-NIV, Pune for their support during the outbreak response. We also acknowledge the excellent technical support from Mrs. Triparna Majumdar, Mrs. Savita Patil, Dr. Rajlaxmi Jain, Ms. Jyoti Yemul, Ms. Pranita Gawande, Ms. Pratiksha Vedpathak, Mrs. Shubhangi Sathe, Ms. Vaishnavi Kumari, Ms. Nandini Shende, Mr. Raj Hawale, Mr. Ajay Kumar, Mr. Yash Joshi for the diagnosis and data management.

References

- Orviz E, Negrodo A, Ayerdi O, et al. Monkeypox outbreak in Madrid (Spain): clinical and virological aspects. *Journal of Infection* 2022 Jul 10.
- Parker S, Nuara A, Buller RM, et al. Human monkeypox: an emerging zoonotic disease. *Future Microbiol* 2007;2(1):17–34.
- WHO. Disease outbreak news; multi-country monkeypox outbreak in non-endemic countries. World Health Organization; 2022 <https://www.who.int/emergencies/disease-outbreak-news/item/2022-DON385> Accessed on July 19, 2022.
- Bunge EM, Hoet B, Chen L, Lienert F, Weidenthaler H, Baer LR, Steffen R. The changing epidemiology of human monkeypox—A potential threat? A systematic review. *PLoS neglected tropical diseases* 2022;16(2):e0010141.
- WHO. Multi-country outbreak of monkeypox. https://cdn.who.int/media/docs/default-source/2021-dha-docs/20220706_monkeypox_external_sitrep_final.pdf?sfvrsn=1b580b3d_4&download=true. Accessed on July 19, 2022.
- Li Y, Olson VA, Laue T, Laker MT, Damon IK. Detection of monkeypox virus with real-time PCR assays. *Journal of Clinical Virology* 2006;36(3):194–203.
- Li Y, Zhao H, Wilkins K, et al. Real-time PCR assays for the specific detection of monkeypox virus West African and Congo Basin strain DNA. *J. Virol Methods*. 2010;169(1):223–7.
- Yadav PD, Nyayanit DA, Shete AM, et al. Complete Genome Sequencing of Kaisodi Virus Isolated from Ticks in India Belonging to Phlebotomus Genus, Family Phlebotomidae. *Ticks Tick Borne Dis* 2019;10(1):23–33.
- WHO. Monkeypox: experts give virus variants new names <https://www.who.int/news/item/12-08-2022-monkeypox--experts-give-virus-variants-new-names>.
- Gigante CM, Korber B, Seabolt MH, et al. Multiple lineages of Monkeypox virus detected in the United States, 2021–2022. *bioRxiv* 2022. doi:10.1101/2022.06.10.495526.
- Luna N, Ramírez AL, Muñoz M, et al. Phylogenomic analysis of the monkeypox virus (MPXV) 2022 outbreak: Emergence of a novel viral lineage? *Travel Medicine and Infectious Disease* 2022;49(102402).

Pragya D. Yadav*[#]

Indian Council of Medical Research-National Institute of Virology,
Pune, Maharashtra, India, Pin-411021

Aravind Reghukumar[#]

The Government Medical College, Thiruvananthapuram, Kerala, India,
Pin-695011

Rima R. Sahay[#]

Indian Council of Medical Research-National Institute of Virology,
Pune, Maharashtra, India, Pin-411021

Sudeep K

The Government Medical College, Kannur Campus Rd, Pariyaram,
Kerala, India, Pin-670503

Anita M. Shete

Indian Council of Medical Research-National Institute of Virology,
Pune, Maharashtra, India, Pin-411021

Aruna Raman

The Government Medical College, Thiruvananthapuram, Kerala, India,
Pin-695011

Pramod VK

The Government Medical College, Kannur Campus Rd, Pariyaram,
Kerala, India, Pin-670503

Priya Abraham

Indian Council of Medical Research-National Institute of Virology,
Pune, Maharashtra, India, Pin-411021

Reshma Benson

The Government Medical College, Thiruvananthapuram, Kerala, India,
Pin-695011

Sarin SM

The Government Medical College, Kannur Campus Rd, Pariyaram,
Kerala, India, Pin-670503

Sreelekshmy Mohandas, Deepak Y. Patil, Abhinendra Kumar
Indian Council of Medical Research-National Institute of Virology,
Pune, Maharashtra, India, Pin-411021

Nivedita Gupta

Indian Council of Medical Research, V. Ramlingaswami Bhawan,
Ansari Nagar, New Delhi, India, Pin-110029

Anuja Elizabeth George

The Government Medical College, Thiruvananthapuram, Kerala, India,
Pin-695011

Neetu Vijay

Indian Council of Medical Research, V. Ramlingaswami Bhawan,
Ansari Nagar, New Delhi, India, Pin-110029

Anuja U, Manjusree Suresh, Ramiz Raja A

The Government Medical College, Thiruvananthapuram, Kerala, India,
Pin-695011

Gajanan N Sapkal

Indian Council of Medical Research-National Institute of Virology,
Pune, Maharashtra, India, Pin-411021

Manasi Ravindranath

The Government Medical College, Kannur Campus Rd, Pariyaram,
Kerala, India, Pin-670503

Sreenath Sreenivasan

The Government Medical College, Thiruvananthapuram, Kerala, India,
Pin-695011

Preethi James

District Surveillance Officer, District Medical Office, Vanchiyorm
Thiruvananthapuram, Kerala, India, Pin- 695035

Shaj MK

District Surveillance Officer, District Surveillance Unit Integrated
Disease Surveillance Project, District Medical Office, Kannur, Kerala,
India, Pin- 670002

*Corresponding author: Dr. Pragya D. Yadav, Scientist 'F' and
Group Leader, Maximum Containment Facility, Indian Council of
Medical Research-National Institute of Virology, Sus Road,
Pashan, Pune, Maharashtra, India Pin-411021. Phone:
+9120-25906911, Fax No. 91-20-25906669
E-mail address: hellopragya22@gmail.com (P.D. Yadav)

[#] Authors have contributed equally and are first author